Experimental Investigation of Electron-Acoustic Waves in Electron Plasmas

Andrey A. Kabantsev*, F. Valentini† and C. Fred Driscoll*

*Department of Physics, University of California at San Diego, La Jolla, CA USA 92093-0319
†Dipt. di Fisica and INFM, Univ. della Calabria, 87036 Rende, Italy

Abstract. Electron-acoustic waves have strong linear Landau damping, but are observed as nonlinear BGK modes in experiments with pure electron plasmas. The waves have phase velocity $v_\phi \approx 1.3\bar{v}$, in agreement with theory, and the longest wavelength BGK states exhibit only relatively weak damping. Shorter wavelength modes exhibit a strong decay instability which can be experimentally controlled.

Keywords: BGK modes, phase space vortices, vortex merger cascade, nonneutral plasmas
PACS: 52.27.Jt; 52.35.fp; 52.35.Sb

INTRODUCTION

Electron-acoustic wave (EAW) solutions of the linearized electrostatic Vlasov equations have usually been ignored due to their huge Landau damping $(\gamma/f > 1)$ on Maxwellian distributions. This strong linear damping follows from the wave phase velocity being comparable to the electron thermal velocity, that is, $v_\phi \equiv 2\pi f/k_z \sim \bar{v}$. However, recent nonlinear theory and simulations [1, 2] found that electron trapping in the EAW electrostatic potential can result in undamped solutions, i.e. long-lived BGK modes. In essence, population of trapped particles makes the electron velocity distribution flat at the wave phase velocity, effectively turning off Landau damping.

The definitive feature of the EAW is that the density perturbation of "slow" electrons (with $v < v_\phi$) is *almost* cancelled by an opposite-sign density perturbation of "fast" electrons (with $v > v_\phi$). Thus, there is negligible electric restoring force. However, the corresponding pressure perturbations from fast and slow particles are vastly different; the restoring forces come mainly from the pressure of the fast electrons, and the mass of slow electrons provides the inertia. Note that this "self-shielding" feature of the density perturbations greatly reduces the wave electric coupling to wall antennas, making the EAW both hard to excite and to detect.

Experimentally, the required flat trapped-particle velocity distribution is obtained when a resonant driving electric field of moderate amplitude is applied to the wall for many trapping periods, i.e. hundreds of wave cycles. However, for the longest standing wave ($m_z = 1$, with $\lambda = L_p/2$) this drive is also resonant with axial bounce motion since $f_{\mathrm{EAW}} \approx 1.3\bar{v}/2L_p \equiv 1.3 f_{\mathrm{bnc}}$. Thus, such drive causes significant bulk plasma heating due to bounce resonances [3], which continuously changes both the electron thermal velocity and the EAW phase velocity.

In fact, it is possible to excite the EAWs at any of a broad range of frequencies above the minimal f_{EAW} by keeping the drive at frequency $f = f_{\mathrm{EAW}} + \delta f$ for a long enough

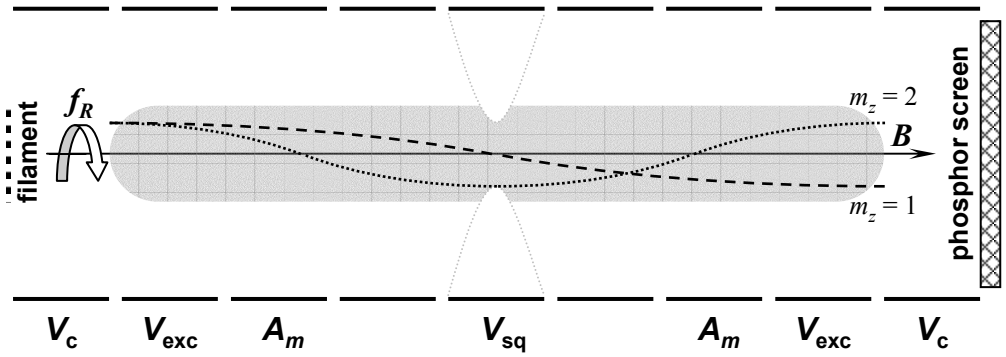

FIGURE 1. Schematic of cylindrical Penning-Malmberg trap with electron plasma and $m_z = 1,2$ plasma waves.

time. Plasma heating then adjusts the thermal velocity and EAW phase velocity to be in resonance with the drive. To minimize the bulk plasma heating, one can excite first the $m_z = 2$ or $m_z = 4$ modes, since much less heating occurs from applied voltages at $f \approx 2.6 f_{\rm bnc}$ or $f \approx 5.2 f_{\rm bnc}$. The rapid EAW decay instability predicted theoretically [2] and observed here then produces the $m_z = 1$ EAW unless the phase-space vortex merging is deliberately suppressed.

EXPERIMENTAL SETUP

In our experiments we use a cylindrical Penning-Malmberg trap [4], shown schematically in Fig. 1. The electron column of length $L_p \leq 50$ cm is contained inside a stack of hollow conducting cylinders of radius $R_w = 3.5$ cm, which reside in an ultrahigh vacuum with residual pressure $\sim 10^{-11}$ Torr. The end cylinders are negatively biased ($V_c = -100$ V) with respect to the central plasma potential ($\phi_{p0} \approx -30$ V) to axially confine electrons. A strong axial magnetic field ($B \leq 20$ kG) ensures radial confinement. These pure electron plasmas have exceptional confinement properties and can be maintained for hours [5].

In equilibrium, typical electron columns have central density $n_0 \approx 1.5 \cdot 10^7$ cm^{-3} over a bell-shaped radial profile with a characteristic radius $R_p \approx 1.2$ cm, giving line density $N_L \equiv n_0 \pi R_p^2 \approx 7 \cdot 10^7$ cm^{-1}. The typical electron temperature is $T_e \sim 1$ eV which gives $\bar{\rm v} \sim 40$ cm/μs, $f_{\rm bnc} \approx 0.4$ MHz, and a Debye length $\lambda_D \approx 0.2$ cm. The unneutralized electron charge results in an $\mathbf{E} \times \mathbf{B}$ rotation of the column at frequency $f_R \sim 0.1\ {\rm MHz}(B/2\ {\rm kG})^{-1}$.

The "evaporative" temperature T_e represents the high energy tail (${\rm v} > 4\bar{\rm v}$) of the electron velocity distribution, since it is obtained from $\sim 1\%$ of the electrons near $r = 0$ which escape past a ramped confinement potential. A new temperature diagnostic which measures *all* escaping particles suggests significantly lower bulk temperatures, which also depend on radius. Thus, quantitative predictions of $f_{\rm EAW}$ and ${\rm v}_\phi$ are not yet possible.

We excite the $m_\theta = 0$ waves by applying a sinusoidally oscillating voltage $V_{\rm exc}$ to the last inner cylinders (next to the confinement cylinders) on both electron column

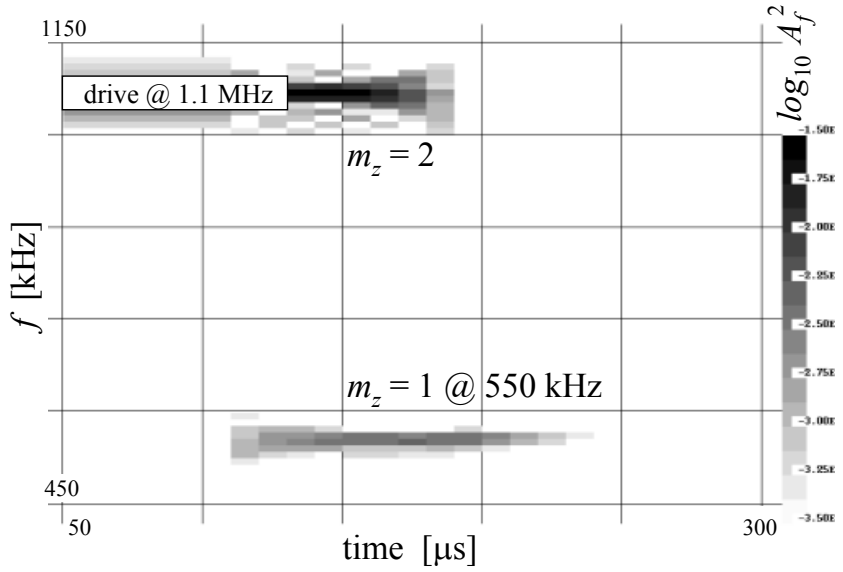

FIGURE 2. EAW's energy density as function of frequency (vertical) and time (horizontal) after $m_z = 2$ wave excitation. $m_z = 2$ decay (merging of the phase space vortices) into $m_z = 1$ starts about 110 μs after the beginning of excitation.

ends. This voltage causes the end sheaths to oscillate in z. When the voltages on the two cylinders have opposite phase, the plasma length stays nearly constant while its center of mass oscillates in z, so the EAW with odd $m_z = 1,3...$ is excited if the driving frequency hits the resonance. In contrast, when the voltages on the two cylinders are in phase, both ends are compressed at the same time, and the EAW with even $m_z = 2,4...$ is excited. This double-end in-phase excitation of even EAWs further minimizes the bounce-resonant heating [3].

The temporal evolutions and damping rates $\gamma_m(t)$ of the $m_\theta = 0$, $m_z = 1,2,3...$ EAWs are measured by digitizing the wall voltages $A_w(t)$ induced on the cylinders just inside the driving cylinders. They are connected in-phase for detection of even m_z modes, and opposite-phase for the odd m_z modes. For simultaneous detection of odd and even modes, a single cylinder at one side of the electron column can be used.

The received waveforms $A_w(t)$ are analyzed with fourier transforms giving spectral amplitudes $A_f(t_j)$ during separate time slices t_j; and by direct fits of A_w to the sums of 2 growing or damping sinusoids. Moreover, the $m_z = 1$ amplitude $A_1(t)$ is calibrated in terms of $\delta n/n$ by comparison to images from a CCD camera diagnostic [6]. Here, the plasma is first cut in half by a negative voltage V_{sq} applied to the central cylinder, so that only *one-half* of the plasma is dumped onto the phosphor screen. Of course, the cut must be done rapidly compared to a wave period to avoid phase-averaging.

The same techniques are used to excite and detect the venerable $m_\theta = 0$, $m_z = 1,2,3$ Trivelpiece-Gould (TG) plasma modes [7]. Long wavelength TG modes also have an

acoustic dispersion relation, but with much higher phase velocity, given by

$$v_\phi^{TG} \approx \left(\frac{2e^2 N_L}{m_e}\ln\frac{R_w}{R_p}\right)^{0.5}\left[1+\frac{3}{2}\left(\frac{\bar{v}}{v_\phi}\right)^2\right] \approx 2\cdot 10^8 \text{ cm/sec} \approx 5\bar{v}. \qquad (1)$$

The measured TG mode frequencies correspond closely to the theory prediction, and only weakly depend on the plasma temperature or wavenumber m_z since $(v_\phi/\bar{v})^2 \gg 1$. In our experiments on the EAWs, these TG modes serve as an independent reference point for the "finger-like" plasma wave dispersion curve that includes both the TG mode (upper) and the EAW (lower) branches [2].

EXPERIMENTAL RESULTS

Figure 2 shows the received spectrum $A_f(t_j)$ of the EAWs after 150 cycles of resonant $m_z = 2$ mode excitation (during $0 < t < 130\mu$s). Even before the $m_z = 2$ excitation stops ($\sim 130\ \mu$sec), the $m_z = 1$ mode ($f \approx 550$ kHz) at half the $m_z = 2$ frequency starts to grow. This $2 \rightarrow 1$ decay causes fast damping of the $m_z = 2$ mode after the drive stops, and the $m_z = 1$ mode then damps due to collisions. Note that the display shows 2 decades in spectral power A_f^2 (from $\log_{10} A_f^2 = -1.5 \rightarrow -3.5$), and no other waves are significant at intervening frequencies.

Figure 3 shows the waveform $A_w(t)$ during this decay instability that effectively transfers energy from mode $m_z = 2$ to mode $m_z = 1$. At maximum amplitude the $m_z = 1$ EAW has peak-to-peak density variations $\delta n^{pp}/n \approx 0.07$, which translates to pressure fluctuations of more than 50% (from fast electrons). Later the $m_z = 1$ EAW exhibits an exponential decay with a rate $\gamma_1 \approx 30\cdot 10^3$ sec^{-1}. This damping is significantly decreased at higher electron temperatures. We speculate that this damping is due to electron-electron collisional restoration of the Maxwellian distribution function.

This $m_z = 2$ to $m_z = 1$ mode decay corresponds to a transition in z-v_z phase space from 2 vortices to 1 vortex. The phase-space vortex merging dynamics can be controlled by applying small potential barriers (or wells) to the wall cylinders between the high m_z wavelengths. Here smallness is in comparison to typical plasma potential $\phi_{p0} \approx -30$ V.

We observe experimentally that a (negative) potential barrier with amplitude $-V_{sq} \sim 2$ V placed on the wall significantly slows the EAW decay to longer wavelengths, and a barrier with amplitude $-V_{sq} \geq 3$ V completely stops the decay. This squeeze is applied 100 μs after the beginning of excitation, right before the high m_z mode has reached its maximum.

Figure 4 shows the received spectrum $A_f(t_j)$ when the squeeze inhibits the decay. Instead of the original fast decay into the $m_z = 1$ EAW (as in Fig. 2), the $m_z = 2$ mode now exhibits only collisional damping. Figure 5 shows exponential decay with $\gamma_2 \sim 30\times 10^3 s^{-1}$, which is the same as γ_1 for the $m_z = 1$ mode. Here further measurements are needed to characterize the full velocity distribution versus radius, since the EAW mode frequencies scale with $\bar{v}$ and incorporate several subtle cancellations.

In contrast, applying positive potential perturbations (attracting wells) to the wall cylinders between the high m_z standing wavelengths, the vortex merging cascade has been significantly accelerated.

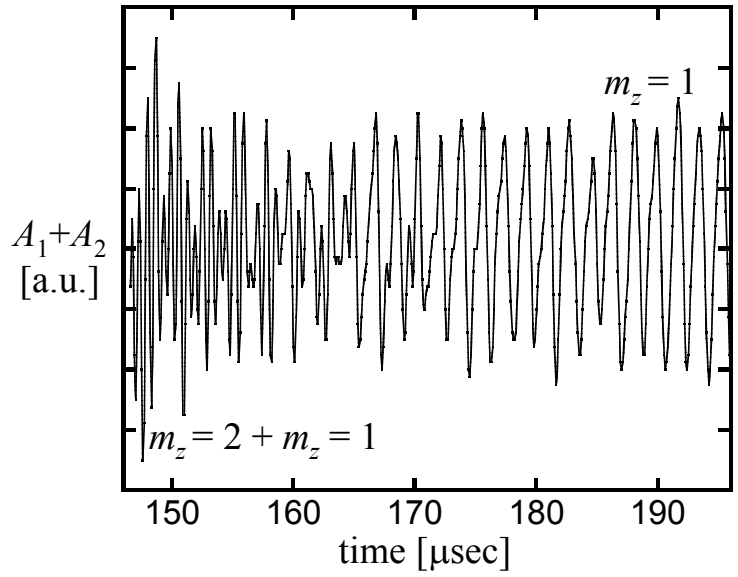

FIGURE 3. Decay instability of the $m_z = 2$ EAW. The merger to a single vortex occurs at a time scale much shorter than the collisional damping of the EAWs.

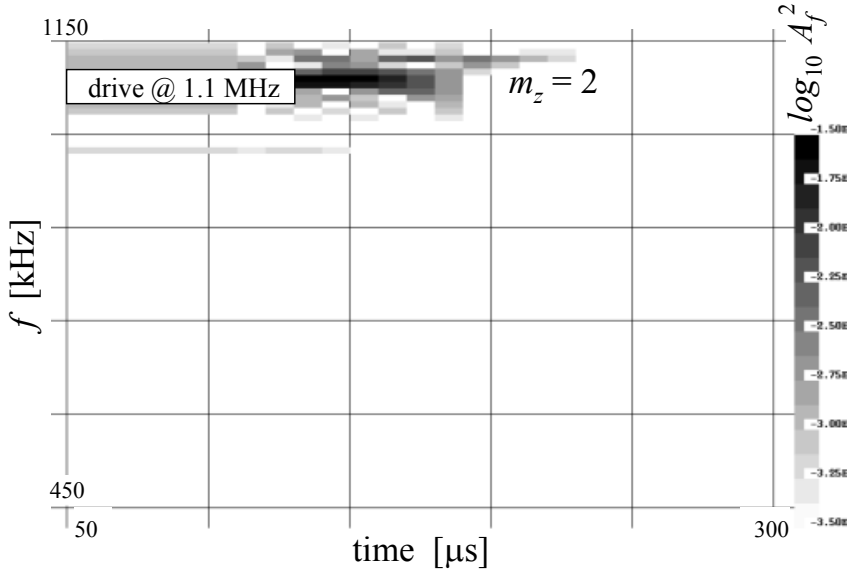

FIGURE 4. EAW's energy density as function of frequency (vertical) and time (horizontal) after $m_z = 2$ wave excitation. Small potential barrier ($V_{sq} = -3\,V$) applied at 100 μs after the beginning of excitation prevents merging of the phase space vortices, thus only collisional decay of $m_z = 2$ is observed.

CONCLUSIONS

Nonlinear electron-acoustic waves and their decay instability are readily observed in nonneutral plasmas. The waves have acoustic dispersion relation with phase velocity

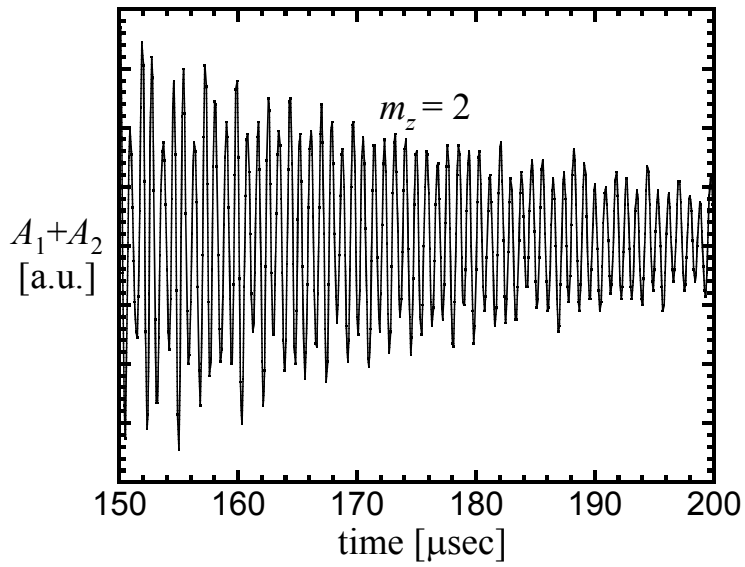

FIGURE 5. Collisional damping of the $m_z = 2$ EAW when its decay to a single vortex is prohibited by $V_{sq} = -3\,\mathrm{V}$.

near the predicted $v_\phi \approx 1.3\bar{v}$. Quantitative predictions of v_ϕ require knowledge of the full distribution function versus radius, which is not yet measured. The longest wavelength mode ($m_z = 1$) exhibits only a relatively weak damping due to electron-electron collisional diffusion of wave-trapped particles. Modes with higher m_z wavenumbers show the predicted fast decay to longer wavelengths. This phase space-vortex merger can be suppressed by applying small potential barriers to the wall between the high m_z vortices. Being prevented from the decay instability, the high m_z modes exhibit the same rate of collisional damping as the $m_z = 1$ mode.

Note added in press: A similar decay instability of Trivelpiece-Gould modes in pure electron plasmas has been well characterized experimentally by H. Higaki [8].

ACKNOWLEDGMENTS

This work was supported by National Science Foundation Grant No. PHY0354979.

REFERENCES

1. J.P. Holloway and J.J. Dorning, *Phys. Rev. A* **44**, 3856-3868 (1991).
2. F. Valentini, T.M. O'Neil and D.H.E. Dubin, *Phys. Plasmas* **13**, 052303 (2006); also "Excitation and Decay of Electron Acoustic Waves," this proceedings.
3. B.P. Cluggish, J.R. Danielson and C.F. Driscoll, *Phys. Rev. Lett.* **81**, 353-356 (1998).
4. C.F. Driscoll and J.H. Malmberg, *Phys. Rev. Lett.* **81**, 167-170 (1998).
5. C.F. Driscoll, K.S. Fine and J.H. Malmberg, *Phys. Fluids* **29**, 2015-2017 (1983).
6. K.S. Fine, A.c. Cass, W.G. Flynn and C.F. Driscoll, *Phys. Rev. Lett.* **75**, 3277-3280 (1995).
7. A.W. Trivelpiece and R.W. Gould, *J. Applied Phys.* **30**, 1784-1793 (1959).
8. H. Higaki, *Plasma Phys. Control. Fusion* **39**, 1793-1803 (1997).